Facile Fabrication of Hybrid Nanoparticles Surface Grafted with Multi-Responsive Polymer Brushes via Block Copolymer Micellization and Self-Catalyzed Core Gelation

YANFENG ZHANG, WEIYIN GU, HANGXUN XU, SHIYONG LIU

Department of Polymer Science and Engineering, Joint Laboratory of Polymer Thin Films and Solution, Hefei National Laboratory for Physical Sciences at the Microscale, University of Science and Technology of China, Hefei, Anhui 230026, China

Received 7 October 2007; accepted 9 December 2007
DOI: 10.1002/pola.22572
Published online in Wiley InterScience (www.interscience.wiley.com).

ABSTRACT: Poly(2-(dimethylamino)ethyl methacrylate)-*b*-poly(γ-methacryloxypropyltrimethoxysilane) (PDMA-*b*-PMPS) was synthesized via consecutive reversible addition-fragmentation chain transfer (RAFT) polymerizations in 1,4-dioxane. Subsequent micellization of the obtained amphiphilic diblock polymer in aqueous solution led to the formation of nanoparticles consisting of hydrophobic PMPS cores and well-solvated PDMA shells. Containing tertiary amine residues, PDMA blocks in micelle coronas can spontaneously catalyze the sol–gel reactions of trimethoxysilyl groups within PMPS cores, leading to the formation of hybrid nanoparticles coated with PDMA brushes. Transmission electron microscopy (TEM) and laser light scattering (LLS) revealed the presence of monodisperse spherical hybrid nanoparticles, and the grafting density of PDMA chains at the surface of nanoparticle cores was estimated to be $\sim$5.8 nm^2/chain. PDMA brushes exhibit dual stimuli-responsiveness, and the swelling/collapse of them can be finely tuned with solution pH and temperatures. The obtained multi-responsive hybrid nanoparticles might find potential applications in fields such as smart devices, recyclable catalysts, and intelligent nanocarriers for drug delivery or gene transfection. © 2008 Wiley Periodicals, Inc. J Polym Sci Part A: Polym Chem 46: 2379–2389, 2008

Keywords: block copolymers; crosslinking; micelles; reversible addition fragmentation chain transfer (RAFT)

INTRODUCTION

Organic/inorganic hybrid nanoparticles have attracted ever-increasing attention,[1–3] because of their intriguing properties associated with inorganic cores (optical, magnetic, and mechanical properties, etc.)[4–11] and polymeric shells (processability, compatibility, stimuli-responsiveness, etc.).[12–16] Because of the ease of particle synthesis, hybrid silica nanoparticles have been most extensively studied. They can be prepared by either physical adsorption or covalent grafting techniques starting from bare silica nanoparticles. The latter involves either the "grafting from"[9,10,12,17–33] or "grafting to"[34–36] approaches. Compared to "grafting to," the "grafting from" approach provides much better control over surface grafting densities and grafted chain lengths,[37] taking advantage of the striding advances recently achieved in the field of controlled/living radical polymerizations, such as atom transfer radical polymerization (ATRP),[12,20–23,28,30] reversible addition-fragmentation chain transfer polymerization (RAFT),[29] and nitroxide-mediated radical polymerization (NMRP).[27,31]

Correspondence to: S. Liu (E-mail: sliu@ustc.edu.cn)

On the other hand, hybrid nanoparticles can also be fabricated via the combination of block copolymer self-assembly[38,39] and subsequent sol–gel reactions of trialkyloxysilyl residues. Fukuda and coworkers[40] prepared silanol surface-functionalized micelles via the self-assembly of amphiphilic ABC triblock copolymers with the hydrophilic block incorporated with protected silanol monomers, γ-methacryloxypropyltrimethoxysilane (MPS). The obtained reactive micelles were then coated with a silica layer via sol–gel reactions. Chen et al.[41] reported the preparation of hybrid core-shell nanoparticles from poly(ethylene oxide)-*b*-poly(γ-methacryloxypropyltrimethoxysilane) (PEO-*b*-PMPS). Bearing reactive PMPS moieties, the self-assembled nanostructures of PEO-*b*-PMPS in water can be covalently fixed via gelation of hydrophobic PMPS cores or bilayers in the presence of weak bases such as triethylamine, leading to the formation of hybrid nanoparticles.

Recent progress in the field of hybrid nanoparticles involves the preparation of inorganic nanoparticles coated with stimuli-responsive polymer brushes, which are attractive building blocks for the design and fabrication of smart nanostructured devices.[42–47] Armes and coworkers[48,49] grafted pH-responsive poly(2-(diethylamino)ethyl methacrylate) (PDEA), and multi-responsive poly(2-(dimethylamino)ethyl methacrylate) (PDMA) and poly(2-(*N*-morpholino)ethyl methacrylate) (PMEMA) brushes at the surface of silica nanoparticles via surface-initiated ATRP. Zhao et al.[30] reported the preparation of thermoresponsive hybrid silica nanoparticles coated with poly(methoxydi(ethylene glycol) methacrylate) or poly(methoxytri(ethylene glycol) methacrylate) brushes. Poly(*N*-isopropylacrylamide) (PNIPAM) has been well-known as a thermoresponsive polymer, exhibiting a lower critical solution temperature (LCST) at $\sim$32 °C.[50] Zhu et al.[51] synthesized gold nanoparticles stabilized with thiol-terminated PNIPAM via the "grafting to" approach. Tenhu and coworkers[52–54] prepared PNIPAM-coated gold nanoparticles using both "grafting to" and "graft from" approaches, and further micro-DSC studies revealed intriguing double thermal phase transitions for PNIPAM brushes.

Previously, we fabricated thermoresponsive hybrid nanoparticles coated with PNIPAM brushes via the self-assembling approach, starting from PNIPAM-*b*-PMPS diblock copolymer prepared via the RAFT process.[55] We also demonstrated that these hybrid nanoparticles can be prepared in a one-pot manner, taking advantage of high monomer conversion during the RAFT polymerization of MPS and the absence of any metal catalysts, which are typically encountered in ATRP.

It should be noted that after the self-assembly of block copolymer in water, the subsequent sol–gel reaction was typically catalyzed by the addition of weak bases such as triethylamine. Recently, Du and Armes[56] reported the preparation of pH-responsive hybrid vesicles from poly(ethylene oxide)-*b*-poly(2-(diethylamino)ethyl methacrylate-*co*-γ-methacryloxypropyl-trimethoxysilane), PEO-*b*-P(DEA-*co*-MPS). The sol–gel reactions within hydrophobic PDEA layers were self-catalyzed by tertiary amine residues of DEA monomer units.

PDMA is a weak polybase and possesses a pK_a of $\sim$7.1. At room temperature, PDMA homopolymer is water-soluble over the whole pH range with considerably lower water solubility at pH $>$ 9–10. Below pH 6–7, PDMA is soluble as a weak cationic polyelectrolyte due to protonation of tertiary amine groups. Above pH 8, PDMA also exhibits LCST phase behavior and phase separates from aqueous solution at $\sim$32–50 °C depending on its molecular weight.[57–59] Moreover, PDMA homopolymers can also act as efficient cationic condensing agents of DNA for gene transfection.[60,61] Thus, hybrid nanoparticles coated with PDMA brushes can combine the advantages of corona multi-responsiveness, encapsulation and controlled release of guest molecules, and complexing agent for DNA delivery.

In this communication, organic/inorganic hybrid nanoparticles coated with multi-responsive PDMA brushes were fabricated via the self-assembly of poly(2-(dimethylamino)ethyl methacrylate)-*b*-poly(γ-methacryloxypropyltrimethoxysilane) (PDMA-*b*-PMPS) in aqueous solution and subsequent self-catalyzed gelation within PMPS cores because of the presence of tertiary amine residues in PDMA blocks. PDMA brushes at the surface of nanoparticle cores exhibit multi-responsiveness to solution pH and temperatures. Transmission electron microscopy (TEM), laser light scattering (LLS), and optical transmittance were employed to characterize the obtained hybrid nanoparticles, and the reversible pH- and thermoresponsive swelling/collapse of PDMA brushes. To the best of our knowledge, this represents the first report on the fabrication of multi-responsive hybrid nanoparticles via the combination of block copolymer self-assembly and self-catalyzed core gelation.

EXPERIMENTAL

Materials

2-(Dimethylamino)ethyl methacrylate (DMA, 99%, Aldrich) was dried over calcium hydride, vacuum-distilled, and then stored at −20 °C prior to use. γ-Methacryloxypropyltrimethoxysilane (MPS, 98%) was purchased from Aldrich and purified by distillation under reduced pressure. 1,4-Dioxane was dried over $LiAlH_4$ and distilled at reduced pressure just prior to use. 2-Cyanopropyl-2-yl dithiobenzoate (CPDB) was synthesized according to literature procedures.[62] 2,2′-Azobisisobutyronitrile (AIBN, 98%, Fluka) was recrystallized from 95% ethanol. *n*-Hexane, toluene, and tetrahydrofuran (THF) were dried by refluxing over sodium and distilled just prior to use. All other chemicals were purchased from Shanghai Chemical Reagent and used as received.

Sample Preparation

RAFT Polymerization of PDMA

A typical polymerization procedure is as follows. A glass ampule was loaded with DMA (8.4 mL, 50 mmol), AIBN (7 mg, 0.043 mmol), CPDB (44 mg, 0.2 mmol), and 1,4-dioxane (6.0 mL). The mixture was degassed through three freeze-pump-thaw cycles. The ampoule was then flame-sealed under vacuum, and immersed into an oil bath thermostated at 70 °C to start the polymerization. After 10 h, the ampule was quenched into liquid nitrogen to stop the polymerization. The reaction mixture was diluted with 1,4-dioxane, and then precipitated into an excess of petroleum ether. This purification cycle was repeated for three times. The obtained product was dried overnight in a vacuum oven at room temperature. The molecular weight and molecular weight distribution were determined by gel permeation chromatography (GPC) using THF as the eluent: M_n = 25,500, M_w/M_n = 1.12. The actual degree of polymerization (DP) of the obtained PDMA was determined to be 230 by ^{1}H-NMR, thus it was denoted as $PDMA_{230}$. Using similar protocols, $PDMA_{48}$ was also prepared. $M_{n,GPC}$ = 6700, M_w/M_n = 1.18. $PDMA_{230}$ and $PDMA_{48}$ were then employed as macro-RAFT agents for the subsequent RAFT block polymerization of MPS monomers.

Synthesis of PDMA-b-PMPS

In a typical procedure, a round-bottom flask equipped with a PTFE stopcock and nitrogen inlet was loaded with $PDMA_{230}$ (1.0 g, 28 μmol dithioester moieties) and 5 mL dry toluene. The macro-RAFT agent was dried by azotropic distillation and then subjected to high vacuum (1×10^{-3} mmHg) for 6 h. Under protection of dry N_2, freshly distilled MPS (1.5 mL, 6.4 mmol), AIBN (1 mg, 6 μmol), and dry 1,4-dioxane (3 mL) were added to the flask. The flask was degassed by three freeze-pump-thaw cycles, and then sealed under vacuum using the PTFE stopcock. The flask was then immersed into an oil bath preheated to 80 °C to start the polymerization. After 20 h, the reaction flask was quenched into liquid nitrogen to stop the polymerization. Under protection of N_2 flow, dry 1,4-dioxane was added to dilute the reaction mixture. An excess of dry *n*-hexane was added under protection of N_2 flow to precipitate out the diblock copolymer. The above purification cycle was repeated for three times. The final product was dried under high vacuum for 6 h, and then directly stored in the reaction flask filled with dry N_2. The molecular weight and molecular weight distribution were determined by GPC: M_n = 43,100, M_w/M_n = 1.32. The actual DP of the PMPS block was determined to be 165 by ^{1}H-NMR. The obtained diblock copolymer was denoted as $PDMA_{230}$-*b*-$PMPS_{165}$. Another diblock copolymer with shorter block lengths, $PDMA_{48}$-*b*-$PMPS_{60}$ was also synthesized according to similar procedures as described earlier. $M_{n,GPC}$ = 21,700, M_w/M_n = 1.26.

Preparation of Hybrid Nanoparticles via Micellization and Self-Catalyzed Gelation

Two methods were employed for the preparation of hybrid nanoparticles. Method 1: 2.0 mL 1,4-dioxane containing 50 mg $PDMA_{230}$-*b*-$PMPS_{165}$ was quickly added into deionized water (18.0 mL) under vigorous stirring. Method 2: under stirring, water was slowly added at a constant rate (~5 s per drop) into 2.0 mL 1,4-dioxane containing 50 mg $PDMA_{230}$-*b*-$PMPS_{165}$, the final content of 1,4-dioxane was 10.0 (v/v) %. In both methods, the aqueous dispersions of hybrid nanoparticles were allowed to stir for 12 h after the addition was finished. 1,4-Dioxane was then removed by dialysis against deionized water for 2 days.

Characterization

Transmission Electron Microscopy

Transmission electron microscopy (TEM) analyses were conducted on a Hitachi 800 transmis-

sion electron microscope at an acceleration voltage of 200 kV. Samples for TEM measurements were prepared by placing 10 μL of aqueous dispersion of hybrid nanoparticles on copper grids coated with thin films of Formvar and carbon successively. No staining was required.

Gel Permeation Chromatography

Molecular weights and molecular weight distributions were determined by gel permeation chromatography (GPC) equipped with Waters 1515 pump and Waters 2414 differential refractive index detector (set at 30 °C). It used a series of three linear Styragel columns HT2, HT4, and HT5 at an oven temperature of 45 °C. The eluent was THF at a flow rate of 1.0 mL/min. A series of low polydispersity polystyrene standards were employed for the GPC calibration.

^{1}H-Nuclear Magnetic Resonance Spectroscopy

^{1}H-Nuclear Magnetic Resonance (^{1}H-NMR) spectra were recorded on a Bruker 300 MHz spectrometer. PDMA and PDMA-*b*-PMPS samples were analyzed in $CDCl_3$ at 25 °C.

Laser Light Scattering

A commercial spectrometer (ALV/DLS/SLS-5022F) equipped with a multi-tau digital time correlator (ALV5000) and a cylindrical 22 mW UNIPHASE He-Ne laser (λ_0 = 632 nm) as the light source was employed for dynamic and static laser light scattering (LLS) measurements. In dynamic LLS, scattered light was collected at a fixed angle of 90° for duration of 15 min. Distribution averages and particle size distributions were computed using cumulants analysis and CONTIN routines. All data were averaged over three measurements.

In static LLS, we can obtain the weight-average molar mass (M_w) and the *z*-average root-mean square radius of gyration ($<R_g^2>^{1/2}$ or written as $<R_g>$) of aggregates in a dilute solution from the angular dependence of the excess absolute scattering intensity, known as Rayleigh ratio $R_{vv}(q)$. The specific refractive index increments (dn/dc) were determined by a precise differential refractometer at 632 nm. The molar mass of hybrid nanoparticles was measured at only one concentration (5×10^{-5} g/mL), and the extrapolation to zero concentration was not conducted. Thus, the obtained M_w should only be considered as apparent values, denoted as $M_{w,app}$.

Optical Transmittance Measurements

The optical transmittance of aqueous solutions of hybrid nanoparticles was acquired at a wavelength of 500 nm on a Unico UV–vis 2802PCS spectrophotometer using a thermostatically controlled couvette.

RESULTS AND DISCUSSION

Synthesis of $PDMA_{230}$-*b*-$PMPS_{165}$

The general approaches to the preparation of $PDMA_{230}$-*b*-$PMPS_{165}$ diblock copolymer were shown in Scheme 1(A). The target block copolymer was synthesized via consecutive RAFT polymerizations of DMA and MPS monomers.

Considering that PMPS homopolymer is very viscous and very tricky to handle,[63] we chose to synthesize PDMA homopolymer via the RAFT technique and then employed it as macro-RAFT agent for the controlled radical polymerization of MPS monomer. ^{1}H-NMR spectrum of PDMA in $CDCl_3$ revealed the presence of characteristic signals at δ = 4.1 (*c*), 2.6 (*d*), and 2.3 ppm (*e*) [Fig. 1 (A)]. A closer examination of the NMR spectrum revealed resonance signals at δ = 7.9, 7.5, and 7.4 ppm, which are ascribed to protons of dithiobenzoyl groups at the PDMA chain end [Scheme 1(A)]. On the basis of integral ratios of resonance peaks characteristic of terminal aromatic protons and peak *c* of PDMA, the DP of PDMA was calculated to be ~230. The obtained homopolymer was denoted $PDMA_{230}$. GPC analysis in THF revealed a mono-modal and quite symmetric peak with an M_n of 25,500 and a polydispersity, M_w/M_n, of 1.12 [Fig. 2 (A)].

The PDMA homopolymer was then employed as the chain transfer agent for the RAFT polymerization of MPS. MPS monomer possesses highly reactive —Si(OCH_3) group and is prone to condensation reactions, so great care should be taken during manipulation. A gradual increase of viscosity of the polymerization mixture can be apparently observed at increasing monomer conversions. The final product can be stored in the solid form under dry N_2 atmosphere.

^{1}H-NMR spectrum of the obtained diblock copolymer in $CDCl_3$ together with the peak assignments were shown in Figure 1(B). Besides signals characteristic of PDMA block, it also revealed the presence of characteristic signals of PMPS at δ = 3.9 (*c*′), 3.6 (*f*′), and 0.7 ppm (*e*′).

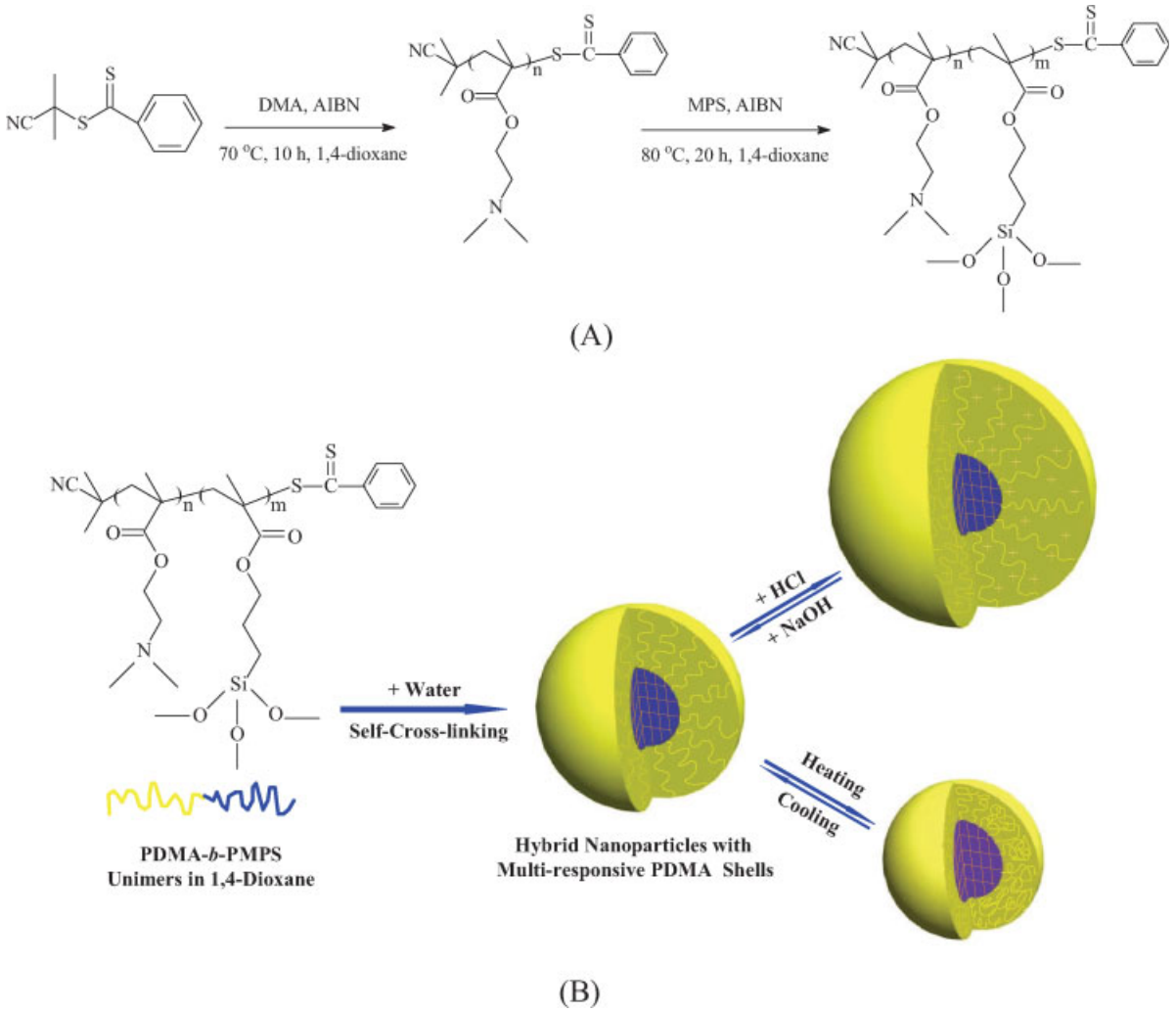

Scheme 1. Schematic illustrations of (A) the preparation of PDMA-*b*-PMPS via RAFT polymerization, and (B) the fabrication of hybrid nanoparticles via block copolymer self-assembly in water, followed by self-catalyzed core gelation. The PDMA corona of hybrid nanoparticles exhibits reversible pH- and thermo-induced swelling/collapse transitions.

Most importantly, characteristic signal of protons in —Si(OCH_3) groups at $\delta = 3.6$ (f') appears as a singlet, indicating that no hydrolysis or condensation reactions occurs during the RAFT polymerization and subsequent purification processes. Moreover, GPC traces in Figure 2 clearly show that the elution peak shifts to higher molecular weight after the polymerization of MPS. The elution peak of PDMA-*b*-PMPS is slightly asymmetric and exhibits no apparent tailing at the lower molecular weight side. On the basis of integral ratios of resonance peaks characteristic of PDMA (c, —COOCH_2—) and PMPS blocks (c', —COOCH_2—), the DP of PMPS block was determined to be 165 by ^{1}H-NMR. Its molecular weight and molecular weight distribution were characterized by GPC in THF: M_n = 43,100, M_w/M_n = 1.32. The obtained diblock copolymer was denoted as $PDMA_{230}$-*b*-$PMPS_{165}$ and used for the subsequent fabrication of hybrid nanoparticles.

Preparation of Hybrid Nanoparticles via Micellization and Self-Catalyzed Core Gelation

PMPS block is hydrophobic and PDMA block is hydrophilic, thus, $PDMA_{230}$-*b*-$PMPS_{165}$ can be considered as amphiphilic diblock copolymer.[64,65] Previously, we fabricated hybrid nanoparticles coated with thermoresponsive PNIPAM brushes,

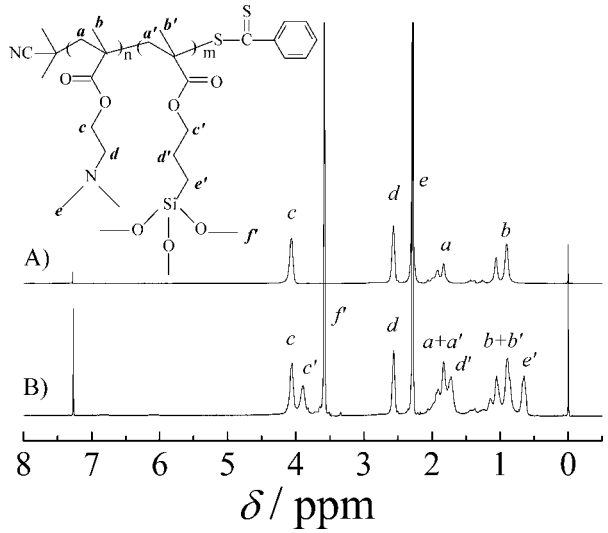

Figure 1. ^{1}H-NMR spectra of (A) $PDMA_{230}$ macro-RAFT agent and (B) $PDMA_{230}$-*b*-$PMPS_{165}$ diblock copolymer in $CDCl_3$.

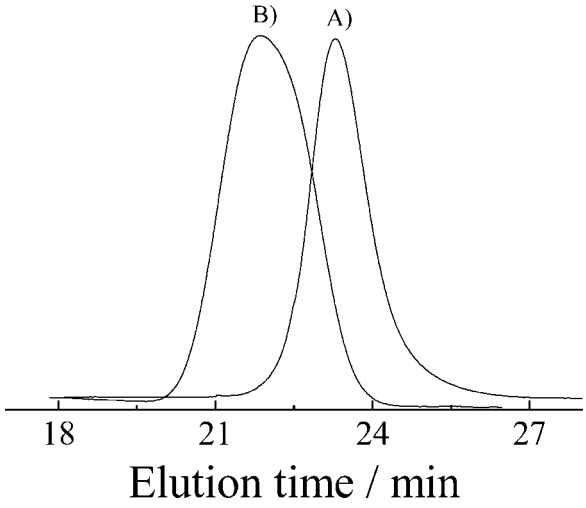

Figure 2. GPC traces of (A) $PDMA_{230}$ macro-RAFT agent (M_n = 25,500, M_w/M_n = 1.12) and (B) $PDMA_{230}$-*b*-$PMPS_{165}$ diblock copolymer (M_n = 43,100, M_w/M_n = 1.32).

starting from PNIPAM-*b*-PMPS.[55] After the micellization in aqueous media, weak base such as triethylamine was added to catalyze the sol–gel reactions within the PMPS cores.

Recently, Du and Armes[56] reported that DEA residues can spontaneously catalyze the sol–gel reactions within vesicles self-assembled from PEO-*b*-P(DEA-*co*-MPS), leading to structurally fixed pH-responsive hybrid capsules. In the current case, as the PDMA block itself is a weak polybase, it might be expected that the fabrication of hybrid nanoparticles can be facilely accomplished via the micellization of $PDMA_{230}$-*b*-$PMPS_{165}$ in water, and that the subsequent sol–gel reactions within hydrophobic PMPS cores can be self-catalyzed by tertiary amine residues in PDMA blocks [Scheme 1(B)].

As the diblock copolymer cannot directly dissolves in water, a cosolvent approach need to be employed. Method 1 employed for the preparation of hybrid nanoparticles involves the quick addition of diblock copolymer solution in 1,4-dioxane into an excess of water under vigorous stirring; whereas in method 2, water was slowly added into the polymer solution in 1,4-dioxane. In both cases, the dispersions after the self-assembly and spontaneous sol–gel reactions possess a bluish tinge, which is characteristic of micellar aggregates of a few tens of nanometers. As aforementioned, because of the presence of tertiary amine residues in PDMA blocks, the subsequent sol–gel reaction can be self-catalyzed by the diblock copolymer, leading to structurally-fixed hybrid nanoparticles coated with PDMA coronas. The successful self-catalyzed core gelation and structural fixation were apparently confirmed by the fact that the bluish tinge can persist upon dilution or addition of a common solvent, DMF, for the original diblock copolymer.

Figure 3 shows typical hydrodynamic radius distribution, $f(R_h)$, obtained for aqueous solutions (pH 10, 25 °C) of self-gelated hybrid nanoparticles prepared by methods 1 and 2. We can

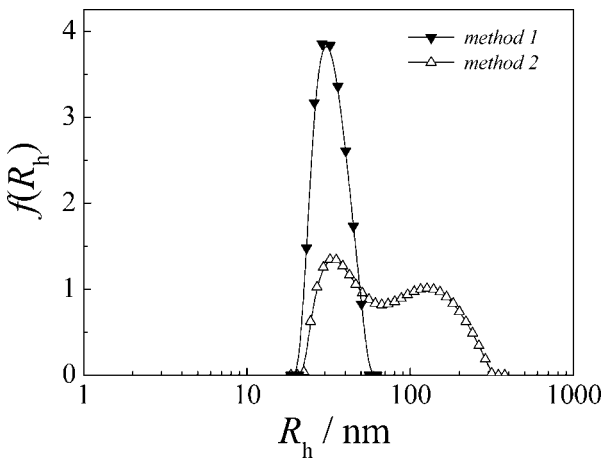

Figure 3. Hydrodynamic radius distribution, $f(R_h)$, obtained for aqueous solutions (pH 10, 25 °C) of self-gelated hybrid nanoparticles prepared from $PDMA_{230}$-*b*-$PMPS_{165}$ via method 1 (▼) and method 2 (△).

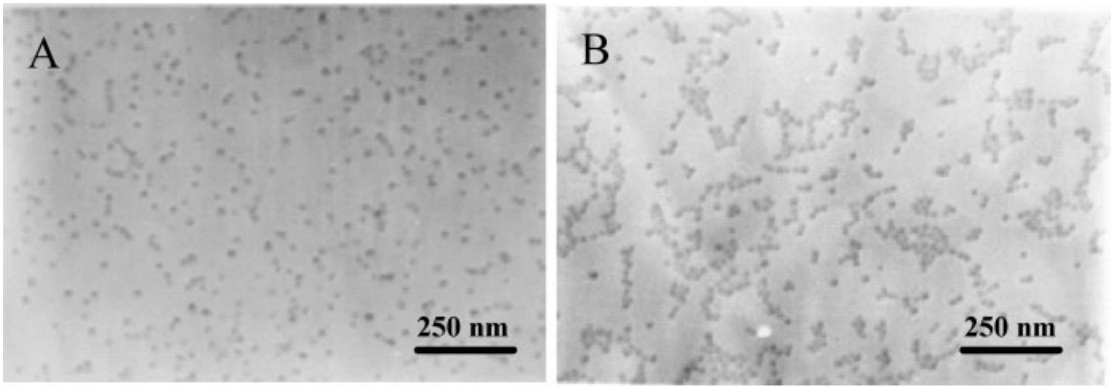

Figure 4. TEM images of self-gelated hybrid nanoparticles prepared from $PDMA_{230}$-*b*-$PMPS_{165}$ via (A) method 1 and (B) method 2.

clearly see that hybrid nanoparticles obtained via method 1 exhibit a mono-modal size distribution, extending from 20 to 60 nm with an intensity-average hydrodynamic radius, $<R_h>$, of 29 nm. These hybrid nanoparticles are relatively narrow-disperse, with a polydispersity index, μ_2/Γ^2, of 0.08. On the other hand, hybrid nanoparticles obtained via method 2 clearly exhibit a bi-modal size distribution, extending from 21 to 320 nm with a $<R_h>$ of 55 nm, and the nanoparticle sizes are relatively polydisperse ($\mu_2/\Gamma^2 = 0.24$).

The obtained hybrid nanoparticles were further characterized by TEM observations (Fig. 4). As silicon element absorbs more of the electron irradiation, the dark region in TEM images should be ascribed to the silica core of hybrid nanoparticles, whereas the PDMA corona chains remain invisible. For hybrid nanoparticles obtained via method 1, TEM image [Fig. 4(A)] reveals the presence of isolated, spherical, and nearly monodisperse nanoparticles, possessing an average size of ~16 nm in diameter. On the contrary, TEM image obtained for hybrid nanoparticles prepared via method 2 mainly reveals fused aggregates of spherical nanoparticles, and isolated nanoparticles only exist as minor fractions. Thus, TEM results were in general agreement with those obtained from LLS, that is, hybrid nanoparticles prepared via method 1 possesses much narrower size distributions and more well-defined microstructures, as compared to that prepared via method 2. Interestingly, closer examinations of TEM images shown in Figure 4 tell us that the sizes of spherical nanoparticles prepared via method 1 are quite comparable to those of small isolated ones obtained via method 2, which is also in agreement with the LLS results (Fig. 3).

It should be noted that method 1 involves abrupt change of solvent quality and the self-assembly immediately occurs after the fast addition of copolymer solution in 1,4-dioxane, whereas in method 2, the solvent quality gradually changes. As there exists a competition between block copolymer self-assembly and self-catalyzed sol–gel reactions, the dramatic effects on morphologies of the final aggregates exerted by the self-assembly procedures is quite expected. In method 1, well-defined nanoparticles possessing PMPS cores and well-solvated PDMA coronas quickly form, and the subsequent self-catalyzed sol–gel reactions within PMPS cores will not lead to interparticle aggregation because of the presence of protective PDMA coronas. In method 2, the self-assembly process actually starts at quite low water contents (~15 v/v %). Thus, the initially formed aggregates do not possess well-defined core-shell microstructures as the volume fraction of 1,4-dioxane is still high, and this will lead to the possible presence of PMPS blocks in the outer part of aggregates. Thus, self-catalyzed sol–gel reactions might between corona PMPS sequences might lead to covalent fusion between aggregates, as revealed by LLS and TEM results shown in Figures 3 and 4. Hybrid nanoparticles prepared via method 1 were then employed for subsequent studies because of its well-defined core-shell microstructure [Scheme 1(B)].

Multi-Responsiveness of Hybrid Nanoparticles Coated with PDMA Brushes

At pH 10 and 25 °C, the intensity-average hydrodynamic radius, $<R_h>$, of hybrid nanoparticles (method 1) fabricated from $PDMA_{230}$-*b*-

$PMPS_{165}$ was determined to be 29 nm by dynamic LLS. As the nanoparticle core size is ~8 nm in radius [TEM results, Fig. 4(A)], the thickness of the PDMA corona can be estimated to be 21 nm. Preliminary experiments revealed that $<R_h>$ value of free PDMA chains with a DP of ~230 in aqueous solutions is ~4–5 nm at pH 10. Thus, the thickness of PDMA corona layers is much larger than the hydrodynamic dimensions (8–10 nm) of free PDMA coils with comparable DPs.

Static LLS measurement of the hybrid nanoparticles at pH 10 and a concentration of 1×10^{-6} g/mL revealed an apparent molar mass, $M_{w,app}$, of 1.2×10^7 g/mol and an average radius of gyration, $<R_g>$, of 23 nm. The number-average molecular weight of $PDMA_{230}$-*b*-$PMPS_{165}$ was calculated to be 77,100. During self-catalyzed gelation within PMPS cores, three $—O_{1/2}CH_3$ groups per MPS repeating units will be lost because of condensation reactions, if we assume that the hydrolysis and crosslinking reactions are 100% complete. After crosslinking, the weight-average molecular weight of per block copolymer chain can be taken as 86,700, considering that the M_w/M_n of diblock copolymer determined by SEC is 1.32. The average aggregation number, N_{agg}, of block copolymer chains inside each hybrid nanoparticles can be estimated to be ~138.

The grafting density of PDMA chains at the surface of nanoparticle cores was then calculated to be 5.8 nm^2/chain. Moreover, the average distance between neighboring grafted PDMA chains at the surface of nanoparticle cores was ~2.4 nm, which is smaller than the hydrodynamic dimensions (8–10 nm) of free PDMA chains at pH 10. As discussed later, at acidic pH, the dimension of PDMA coils will dramatically increase due to protonation of tertiary amine residues. Comparisons of the dimensions (8–10 nm, pH 10) of free PDMA chains with the thickness of PDMA corona layers (21 nm, pH 10), and with the average distance (2.4 nm) between neighboring grafting sites at the surface of nanoparticle cores all suggest that the grafted PDMA layer falls into the brush regime.[37,66] PDMA chains in the brushes are crowded and forced to stretch away from the substrate due to steric exclusion between neighboring chains [Scheme 1(B)].

PDMA homopolymer is multi-responsive, and its water-solubility and chain conformations can vary considerably depending on solution pH and

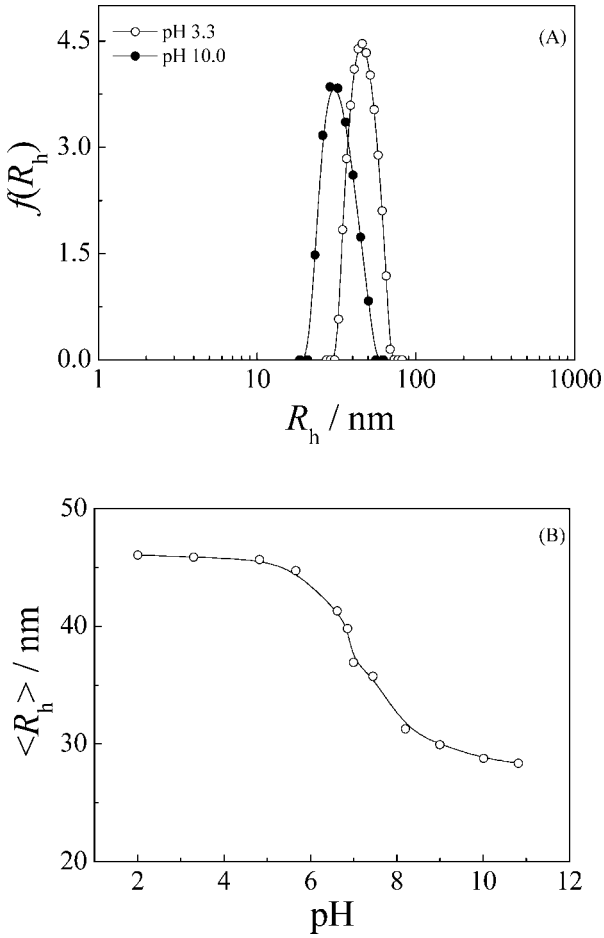

Figure 5. (A) Hydrodynamic radius distributions, $f(R_h)$, at pH 3.3 and 10.0, and (B) pH-dependence of intensity-average hydrodynamic radius, $<R_h>$, obtained at 25 °C for 5.0×10^{-5} g/mL aqueous solutions of self-gelated hybrid nanoparticles prepared from $PDMA_{230}$-*b*-$PMPS_{165}$ via method 1.

temperatures. Figure 5(A) shows typical hydrodynamic radius distributions, $f(R_h)$, obtained for aqueous solutions of hybrid nanoparticles (method 1) at different pH. At pH 3.3, R_h of the hybrid nanoparticles ranges from 30 to 75 nm with $<R_h>$ of 46 nm. Apparently, the hydrodynamic dimension of hybrid nanoparticles at pH 3.3 is much larger than that at pH 10 [Scheme 1(B)].

Figure 5(B) shows the pH dependence of $<R_h>$ obtained for hybrid nanoparticles. $<R_h>$ exhibit a decrease from 46 to 28 nm upon pH increase from 2 to 11. We can also tell from Figure 5(B) that the most dramatic decrease of $<R_h>$ occurs in the narrow pH range of 6–8, which is generally consistent with the pK_a of PDMA blocks (~7.1). Below pH 6, PDMA blocks

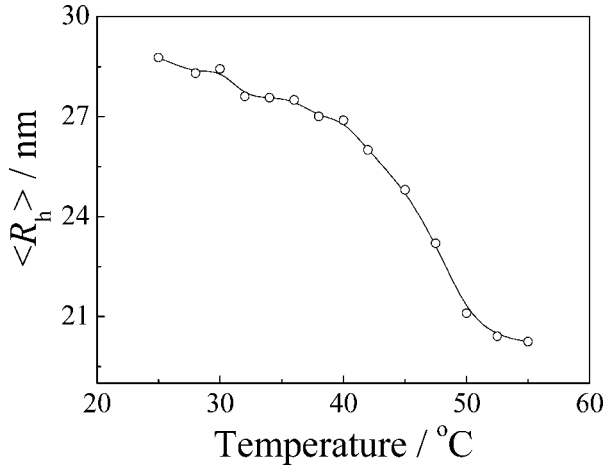

Figure 6. Temperature-dependence of intensity-average hydrodynamic radius, $<R_h>$, obtained for 1.0 $\times$ 10^{-6} g/mL aqueous solution (pH 10) of self-gelated hybrid nanoparticles prepared from $PDMA_{230}$-*b*-$PMPS_{165}$ via method 1.

exist as cationic polyelectrolyte because of the complete protonation of tertiary amine residues. The presence of positive charges along PDMA chain segments will render them to take a more stretched conformation, leading to the prominent increase of $<R_h>$ upon protonation [Scheme 1(B)]. Above pH 8, deprotonation of PDMA brushes results in hybrid nanoparticles with much smaller hydrodynamic dimensions. If should be noted that further LLS studies reveal that pH-induced swelling/collapse of PDMA brushes are fully reversible upon cycling between acidic and alkaline conditions.

PDMA homopolymers in alkaline media (pH > 8) also exhibit LCST phase transitions at ~32–50 °C depending on their molecular weights.[58,59,67–69] We can then expect that PDMA brushes at the surface of nanoparticle cores will also be thermoresponsive [Scheme 1(B)]. Figure 6 shows the temperature dependence of $<R_h>$ of the hybrid nanoparticles at pH 10. Each data point was obtained after the measured values were stable. Upon heating, $<R_h>$ decrease monotonically from 29 nm to 20 nm in the temperature range of 25–55 °C. We can estimate that the hydrodynamic volumes of hybrid nanoparticles shrink for ~3 times upon heating [Scheme 1(B)]. A closer examination of Figure 6 further reveals that the thermo-induced collapse of PDMA brushes occurs in the broad temperature range of 25–50 °C, and the most dramatic decrease of $<R_h>$ takes place in the range 40–50 °C. It should be noted the thermal phase transitions of PDMA homopolymers typically spanned a relatively broad temperatures, which differs from that of PNIPAM homopolymers.[58,59,67–69]

Figure 7 shows the temperature dependence of optical transmittance at a wavelength of 500 nm obtained for the aqueous solution of hybrid nanoparticles coated with PDMA brushes. A much higher concentration (5.0 $\times$ 10^{-4} g/mL) was employed to have good detection sensitivity. The optical transmittance exhibits no changes in the temperature range of 20–35 °C, where LLS results already reveal the collapse of PDMA brushes, probably due to the inner zone of brushes possessing higher chain densities [Fig. 6(B)].[15] Above 35 °C, transmittance decreases abruptly from 88% to ~12% in the temperature range of 35–55 °C due to the aggregation of hybrid nanoparticles because PDMA brushes get insoluble above its thermal phase transition temperature. On the other hand, hybrid nanoparticles prepared from $PDMA_{48}$-*b*-$PMPS_{60}$ via method 1 possess an average hydrodynamic radius, $<R_h>$, of 17 nm (pH 10), which is much smaller than that self-assembled from $PDMA_{230}$-*b*-$PMPS_{165}$. However, hybrid nanoparticles of $PDMA_{48}$-*b*-$PMPS_{60}$ do not exhibit any thermoresponsiveness. At a concentration of 5.0 $\times$ 10^{-4} g/mL, the transmittance remains at ~92% in the temperature range of 20–75 °C. This is probably due to that the DP of PDMA corona chains is relatively low.[55,70]

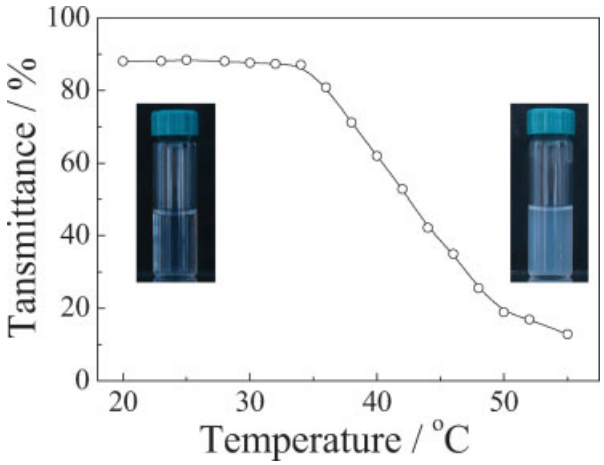

Figure 7. Temperature dependence of optical transmittance at a wavelength of 500 nm obtained for 5.0 $\times$ 10^{-4} g/mL aqueous solution (pH 10) of self-gelated hybrid nanoparticles prepared from $PDMA_{230}$-*b*-$PMPS_{165}$ via method 1.

CONCLUSIONS

In summary, near-monodisperse organic/inorganic hybrid nanoparticles grafted with multi-responsive poly(2-(dimethylamino)ethyl methacrylate) (PDMA) brushes were prepared via the combination of block copolymer self-assembly in aqueous solution and subsequent self-catalyzed sol–gel reactions of trimethoxysilyl residues within micelle cores. PDMA brushes of the obtained hybrid nanoparticles exhibit both pH- and thermoresponsive collapse/swelling transitions, accompanied with solubility changes in aqueous solution. The reported multi-responsive hybrid nanoparticles might find potential applications in the fields of smart nanostructured devices with complex functions, recyclable catalysts, and nanocarriers for encapsulation and controlled release of guest molecules, and condensing agent of DNA for gene transfection.

This work was financially supported by an Outstanding Youth Fund (50425310) and research grants (20534020 and 20674079) from the National Natural Scientific Foundation of China (NNSFC), the "Bai Ren" Project of the Chinese Academy of Sciences, and the Program for Changjiang Scholars and Innovative Research Team in University (PCSIRT).

REFERENCES AND NOTES

1. Hawker, C. J.; Wooley, K. L. Science 2005, 309, 1200.
2. Chen, T.; Colver, P. J.; Bon, S. A. F. Adv Mater 2007, 19, 2286.
3. Beaune, G.; Dubertret, B.; Clement, O.; Vayssettes, C.; Cabuil, V.; Menager, C.; Angew Chem Int Ed 2007, 46, 5421.
4. Wu, K. H.; Shin, M.; Yang, C. C.; Ho, W. D.; Hsu, J. S. J Polym Sci Part A: Polym Chem 2006, 44, 2657.
5. Golden, J. H.; Deng, H. B.; Disalvo, F. J.; Frechet, J. M. J.; Thompson, P. M. Science 1995, 268, 1463.
6. Alivisatos, A. P. Science 1996, 271, 933.
7. Daniel, M. C.; Astruc, D. Chem Rev 2004, 104, 293.
8. Qiao, X. G.; Chen, M.; Zhou, J.; Wu, L. M. J Polym Sci Part A: Polym Chem 2007, 45, 1028.
9. Garcia, I.; Zafeiropoulos, N. E.; Janke, A.; Tercjak, A.; Eceiza, A.; Stamm, M.; Mondragon, I. J Polym Sci Part A: Polym Chem 2007, 45, 925.
10. Gravano, S. M.; Dumas, R.; Liu, K.; Patten, T. E. J Polym Sci Part A: Polym Chem 2005, 43, 3675.
11. Montagne, F.; Mondain-Monval, O.; Pichot, C.; Elaissari, A. J Polym Sci Part A: Polym Chem 2006, 44, 2642.
12. Pyun, J.; Matyjaszewski, K. Chem Mater 2001, 13, 3436.
13. Zhang, H.; Wang, C. L.; Li, M. J.; Zhang, J. H.; Lu, G.; Yang, B. Adv Mater 2005, 17, 853.
14. Brennan, J. L.; Hatzakis, N. S.; Tshikhudo, T. R.; Dirvianskyte, N.; Razumas, V.; Patkar, S.; Vind, J.; Svendsen, A.; Nolte, R. J. M.; Rowan, A. E.; Brust, M. Bioconjugate Chem 2006, 17, 1373.
15. Luo, S. Z.; Xu, J.; Zhang, Y. F.; Liu, S. Y.; Wu, C. J Phys Chem B 2005, 109, 22159.
16. Xu, H. X.; Xu, J.; Jiang, X. Z.; Zhu, Z. Y.; Rao, J. Y.; Yin, J.; Wu, T.; Liu, H. W.; Liu, S. Y. Chem Mater 2007, 19, 2489.
17. Kotal, A.; Mandal, T. K.; Walt, D. R. J Polym Sci Part A: Polym Chem 2005, 43, 3631.
18. Prucker, O.; Ruhe, J. Macromolecules 1998, 31, 592.
19. Prucker, O.; Ruhe, J. Macromolecules 1998, 31, 602.
20. Pyun, J.; Kowalewski, T.; Matyjaszewski, K. Macromol Rapid Commun 2003, 24, 1043.
21. Ohno, K.; Morinaga, T.; Koh, K.; Tsujii, Y.; Fukuda, T. Macromolecules 2005, 38, 2137.
22. von Werne, T.; Patten, T. E. J Am Chem Soc 1999, 121, 7409.
23. von Werne, T.; Patten, T. E. J Am Chem Soc 2001, 123, 7497.
24. Kim, K. M.; Keum, D. K.; Chujo, Y. Macromolecules 2003, 36, 867.
25. Mori, H.; Seng, D. C.; Zhang, M. F.; Muller, A. H. E. Langmuir 2002, 18, 3682.
26. Carrot, G.; Rutot-Houze, D.; Pottier, A.; Degee, P.; Hilborn, J.; Dubois, P. Macromolecules 2002, 35, 8400.
27. Bartholome, C.; Beyou, E.; Bourgeat-Lami, E.; Chaumont, P.; Zydowicz, N. Macromolecules 2003, 36, 7946.
28. Perruchot, C.; Khan, M. A.; Kamitsi, A.; Armes, S. P.; von Werne, T.; Patten, T. E. Langmuir 2001, 17, 4479.
29. Li, C. Z.; Benicewicz, B. C. Macromolecules 2005, 38, 5929.
30. Li, D. J.; Jones, G. L.; Dunlap, J. R.; Hua, F. J.; Zhao, B. Langmuir 2006, 22, 3344.
31. Parvole, J.; Laruelle, G.; Guimon, C.; Francois, J.; Billon, L. Macromol Rapid Commun 2003, 24, 1074.
32. Ueda, J.; Yamaguchi, H.; Yamauchi, T.; Tsubokawa, N. J Polym Sci Part A: Polym Chem 2007, 45, 1143.
33. Ramakrishnan, A.; Dhamodharan, R.; Ruhe, J. J Polym Sci Part A: Polym Chem 2006, 44, 1758.
34. Mansky, P.; Liu, Y.; Huang, E.; Russell, T. P.; Hawker, C. Science 1997, 275, 1458.
35. Lindenblatt, G.; Schartl, W.; Pakula, T.; Schmidt, M. Macromolecules 2000, 33, 9340.
36. Ranjan, R.; Brittain, W. J. Macromolecules 2007, 40, 6217.
37. Zhao, B.; Brittain, W. J Prog Polym Sci 2000, 25, 677.

38. O'Reilly, R. K.; Joralemon, M. J.; Wooley, K. L.; Hawker, C. J. Chem Mater 2005, 17, 5976.
39. Perkin, K. K.; Turner, J. L.; Wooley, K. L.; Mann, S. Nano Lett 2005, 5, 1457.
40. Koh, K.; Ohno, K.; Tsujii, Y.; Fukuda, T. Angew Chem Int Ed Engl 2003, 42, 4194.
41. Chen, Y. M.; Du, J. Z.; Xiong, M.; Zhang, K.; Zhu, H. Macromol Rapid Commun 2006, 27, 741.
42. Ionov, L.; Sapra, S.; Synytska, A.; Rogach, A. L.; Stamm, M.; Diez, S. Adv Mater 2006, 18, 1453.
43. Willner, I.; Basnar, B.; Willner, B. Adv Funct Mater 2007, 17, 702.
44. Barbosa, P. C.; Silva, M. M.; Smith, M. J.; Goncalves, A.; Fortunato, E. Electrochim Acta 2007, 52, 2938.
45. Lecommandoux, S.; Sandre, O.; Checot, F.; Perzynski, R. Prog Solid State Chem 2006, 34, 171.
46. Li, J.; Liu, B.; Li, J. H. Langmuir 2006, 22, 528.
47. Sanchez, C.; Julian, B.; Belleville, P.; Popall, M. J Mater Chem 2005, 15, 3559.
48. Chen, X. Y.; Armes, S. P. Adv Mater 2003, 15, 1558.
49. Du, J. Z.; Chen, Y. M. Angew Chem Int Ed Engl 2004, 43, 5084.
50. Schild, H. G. Prog Polym Sci 1992, 17, 163.
51. Zhu, M. Q.; Wang, L. Q.; Exarhos, G. J.; Li, A. D. Q. J Am Chem Soc 2004, 126, 2656.
52. Raula, J.; Shan, J.; Nuopponen, M.; Niskanen, A.; Jiang, H.; Kauppinen, E. I.; Tenhu, H. Langmuir 2003, 19, 3499.
53. Shan, J.; Chen, J.; Nuopponen, M.; Tenhu, H. Langmuir 2004, 20, 4671.
54. Shan, J.; Nuopponen, M.; Jiang, H.; Kauppinen, E.; Tenhu, H. Macromolecules 2003, 36, 4526.
55. Zhang, Y. F.; Luo, S. Z.; Liu, S. Y. Macromolecules 2005, 38, 9813.
56. Du, J. Z.; Armes, S. P. J Am Chem Soc 2005, 127, 12800.
57. Butun, V.; Billingham, N. C.; Armes, S. P. J Am Chem Soc 1998, 120, 11818.
58. Vamvakaki, M.; Billingham, N. C.; Armes, S. P. Macromolecules 1999, 2088, 32.
59. Xu, J.; Luo, S. Z.; Shi, W. F.; Liu, S. Y. Langmuir 2006, 22, 989.
60. Rungsardthong, U.; Deshpande, M.; Bailey, L.; Vamvakaki, M.; Armes, S. P.; Garnett, M. C.; Stolnik, S. J Controlled Release 2001, 73, 359.
61. Licciardi, M.; Tang, Y.; Billingham, N. C.; Armes, S. P. Biomacromolecules 2005, 6, 1085.
62. Chong, Y. K.; Krstina, J.; Le, T. P. T.; Moad, G.; Postma, A.; Rizzardo, E.; Thang, S. H. Macromolecules 2003, 36, 2256.
63. Mellon, W.; Rinaldi, D.; Bourgeat-Lami, E.; D'Agosto, F. Macromolecules 2005, 38, 1591.
64. Liu, S. Y.; Jiang, M. Chem J Chin Univ-Chin 2001, 22, 1066.
65. Zhu, H.; Liu, S. Y.; Pan, Q. M.; Duan, H. W.; Jiang, M. Chem J Chin Univ-Chin 2002, 23, 138.
66. Halperin, A.; Tirrell, M.; Lodge, T. P. Adv Polym Sci 1992, 100, 31.
67. Butun, V.; Billingham, N. C.; Armes, S. P.; Chem Commun 1997, 671.
68. Vamvakaki, M.; Unali, G. F.; Butun, V.; Boucher, S.; Robinson, K. L.; Billingham, N. C.; Armes, S. P. Macromolecules 2001, 34, 6839.
69. Butun, V.; Armes, S. P.; Billingham, N. C. Polymer 2001, 42, 5993.
70. Zhu, X.; Yan, C.; Winnik, F. M.; Leckband, D. Langmuir 2007, 23, 162.